Study of Pulse Electrochemical Machining of Nickel-Cobalt Ferrous Alloy

D. Bähre[1], O. Weber[2], A. Rebschläger[2], P. Steuer[2]
[1]Institute of Production Engineering, Saarland University, Saarbrücken, Germany
[2]Center for Mechatronics and Automatization, Saarbrücken, Germany

Abstract
In this study, the potential of Pulse Electrochemical Machining (PECM) for the machining of a nickel-cobalt ferrous controlled expansion alloy (Kovar) is investigated. As an alternative procedure to conventional manufacturing technologies like turning, milling or grinding, PECM can be applied to machine this material. The geometry of the cathode is reproduced on the workpiece by electrolytic material removing without any contact with the tool. Therefore, the material removal characteristics of Kovar with PECM are determined by performing systematic design of experiments techniques applying an industrial PECM machine system (PEMCenter8000) to fulfil the effective utilization of the process and to minimize the number of trials. An analysis of the precision of the manufactured geometries and the possibility of generating defined surface qualities are contents of this study.

Keywords
Pulse Electrochemical Machining (PECM), Nickel-Cobalt Ferrous Alloy, Analysis of Variance

1 INTRODUCTION

Pulse Electrochemical Machining (PECM) is an unconventional procedure combining pulsed current and pulsed electrode feed rate (Figure 1), which is very suitable for high precision production in series manufacturing. The main advantage compared to conventional electrochemical processes is that the current pulse is only triggered at the bottom dead centre. This allows for reaching smaller gaps compared to other electrochemical processes, leading to more accuracy [1]. Besides, the electrolyte in the interelectrode gap is refreshed by a chemical product free electrolyte during the pulse off-time leading to better process stability.

Kovar, also known by the brand names Dilvar P1 or Pernifer 2918, is a controlled expansion alloy that matches both borosilicate glasses and alumina ceramics characteristics, making it one of the most popular of the controlled expansion alloys for hermetic sealing or deep-drawing. Furthermore, Kovar is also used in applications such as power tubes, microwave tubes, transistors, diodes, hybrid packages and other scientific instruments. However, conventional manufacturing is very difficult because the material is resilient and mild. The tools tend to plow the alloy instead of cutting into it [2].

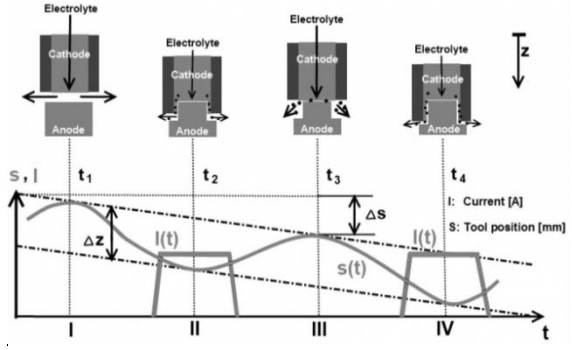

Figure 1 - Pulse Electrochemical Machining principle

Although a few attempts of understanding the mechanisms of the pulse electrochemical machining process have been reported [3], [4], [5], a comprehensive modelling and analysis of the machining characteristics are needed to raise the technical knowledge desired by industrials.

Therefore, the present paper emphasizes features of the development of comprehensive mathematical models for correlating the linear and interaction influences of the various machining parameters (applied voltage, pulse on-time, vibration frequency of the tool, feed rate and electrolyte pressure) on the metal removal rate (MRR) and surface roughness (R_a), for achieving controlled PECM and an optimal selection of process parameters in order to reduce the product development phase. The investigations into the influence of these parameters have been carried out by developing mathematical models based on the design of experiments methodology approach [6], [7].

2 EXPERIMENTAL SET-UP

The chemical composition of the used nickel-cobalt ferrous alloy is shown in Table 1.

C	*Ni*	*Mn*	*Si*	*Co*	*Fe*
0.05	28.3	0.5	0.3	17.4	balance

Table 1 - Kovar composition

The dimensions of the tube-shaped specimens were 19mm in diameter and 30mm in height. They were drilled by a central hole of 7mm in diameter which

enables an inside-out electrolyte flushing. All samples were grinded before the measuring to maintain the surface roughness R_a=0.8µm. The working surface of the cathode made of stainless steel had been electrochemically machined in advance to provide for the roughness R_a=0.1µm. The experiments were conducted on an industrial PEMCenter8000 (Figure 2) from the company PEMTec SNC in Forbach (France). The electrolyte was axially fed to the processing zone through the workpiece. The electrolyte used for the experiments was a solution of $NaNO_3$ with a concentration of 8% and a conductivity of 65mS/cm. The machining was carried out for a fixed time interval of 120s and an initial working gap of 30µm. The material removal rate was determined by measuring the mass loss on a precision balance and the surface roughness with a profilometer MarSurf XR/XT 20.

Figure 2 - PEMCenter8000

3 DESIGN OF EXPERIMENTS

The design of experiments used for analyzing the influence of the fundamental process parameters (applied voltage, pulse on-time, tool vibration frequency, feed rate and electrolyte pressure) on the machining characteristics (MRR and R_a) is proposed according to Siebertz, Bebber and Hochkirchen [6]. The experimentation scheme consists of a 2^k factorial plan, in which *k* is the number of parameters, with the aim to study both the parameter effects and their interactions.

For those five process variables, the design requires 32 experiments distributed in 32 factorial points. The experimental plan was generated and analyzed with the statistical software Minitab 16. The original values of experimental parameters in this set of trials are shown in Table 2. The parameter levels were chosen so that each parameter combination of the experimental plan provides for a stable process.

Parameters	Symbol	Levels	
		-1	1
Voltage (V)	X_1	9	13
Pulse on-time (ms)	X_2	2.9	4.1
Frequency (Hz)	X_3	46	54
Feed rate (mm/min)	X_4	0.07	0.15
Pressure (bar)	X_5	2.50	4.50

Table 2 - Original values of experimental parameters and their coded levels

Trial	X_1	X_2	X_3	X_4	X_5	MRR (g/min)	R_a (µm)
1	-1	-1	-1	-1	-1	0.1222	0.1243
2	1	-1	-1	-1	-1	0.1353	0.1071
3	-1	1	-1	-1	-1	0.1344	0.1416
4	1	1	-1	-1	-1	0.1567	0.1592
5	-1	-1	1	-1	-1	0.1180	0.1494
6	1	-1	1	-1	-1	0.1542	0.1559
7	-1	1	1	-1	-1	0.1236	0.1292
8	1	1	1	-1	-1	0.1595	0.1675
9	-1	-1	-1	1	-1	0.2303	0.1928
10	1	-1	-1	1	-1	0.2795	0.1568
11	-1	1	-1	1	-1	0.2700	0.1430
12	1	1	-1	1	-1	0.2902	0.1301
13	-1	-1	1	1	-1	0.2451	0.1472
14	1	-1	1	1	-1	0.2818	0.1254
15	-1	1	1	1	-1	0.2198	0.0988
16	1	1	1	1	-1	0.3115	0.1168
17	-1	-1	-1	-1	1	0.1033	0.1256
18	1	-1	-1	-1	1	0.1499	0.1344
19	-1	1	-1	-1	1	0.1328	0.1289
20	1	1	-1	-1	1	0.1466	0.1818
21	-1	-1	1	-1	1	0.1093	0.1533
22	1	-1	1	-1	1	0.1337	0.1510
23	-1	1	1	-1	1	0.1199	0.1316
24	1	1	1	-1	1	0.1772	0.2674
25	-1	-1	-1	1	1	0.2645	0.1744
26	1	-1	-1	1	1	0.2550	0.1544
27	-1	1	-1	1	1	0.2470	0.1408
28	1	1	-1	1	1	0.3083	0.1783
29	-1	-1	1	1	1	0.2563	0.1305
30	1	-1	1	1	1	0.3010	0.1308
31	-1	1	1	1	1	0.2433	0.1012
32	1	1	1	1	1	0.2809	0.1517

Table 3 - Experimental design matrix and results

4 MATHEMATICAL MODELLING

The design of experiments methodology is a procedure for analyzing the relationship between the process variables and the responses. By using a factorial plan, these are mathematically fitted by first-order polynomials which enable the evaluation of the parametric effects of the process parameters and their interactions on the investigated machining criteria. Those polynomials can be developed as follows:

$$Y = b_0 + \sum_{i=1}^{k} b_i \cdot X_i + \sum_{i \neq j}^{k} b_{ij} \cdot X_i \cdot X_j \qquad (1)$$

Y represents the corresponding response and X_i are coded levels of quantitative variables. The coefficient b_0 is the constant term and the coefficients b_i and b_{ij} are respectively the linear and interaction terms estimated by applying the least square technique using the observations collected through the design points.

4.1 Mathematical modelling of MRR

Based on Eq. (1) and using the results presented in Table 3, the mathematical relationship for

Source of variation	Degrees of freedom	Sum of squares		Mean sum of squares		F-value	
		MRR	R_a	MRR	R_a	MRR	R_a
Linear	5	0.150441	0.003988	0.030088	0.000798	127.31	3.53
Interaction	10	0.001883	0.023103	0.000188	0.002310	0.80	10.21
Error	16	0.003781	0.003620	0.000236	0.000226		
Total	31	0.156106	0.030711				

Table 4 - Analysis of variance for material removal rate (MRR) and surface roughness (R_a)

correlating the MRR (in g/min) and the considered process parameters was obtained as follows:

$$MRR = 0.2019 + 0.0182X_1 + 0.0057X_2 + 0.0003X_3 + 0.0659X_4 - 0.0001X_5 + 0.0031X_1X_2 + 0.0046X_1X_3 + 0.0026X_1X_4 - 0.0009X_1X_5 - 0.0034X_2X_3 - 0.0021X_2X_4 - 0.0005X_2X_5 - 0.0006X_3X_4 + 0.0006X_3X_5 + 0.0019X_4X_5 \quad (2)$$

4.2 Mathematical modelling of R_a

A comprehensive model based on Eq. (1) has been developed to correlate the interaction of the effects of the previously mentioned process parameters on the R_a criteria (in µm). The mathematical relationship obtained for analyzing the influences of the dominant machining parameters is given by:

$$R_a = 0.1463 + 0.0080X_1 + 0.0017X_2 - 0.0021X_3 - 0.0042X_4 + 0.0060X_5 + 0.0131X_1X_2 + 0.0061X_1X_3 - 0.0070X_1X_4 + 0.0085X_1X_5 - 0.0004X_2X_3 - 0.0112X_2X_4 + 0.0063X_2X_5 - 0.0147X_3X_4 + 0.0020X_3X_5 - 0.0028X_4X_5 \quad (3)$$

5 ANALYSIS AND OPTIMIZATION OF THE DEVELOPED MODELS

The analysis of variance (ANOVA) and the F-ratio test have been performed to identify the machining parameters and the interactions which have significant influence on the investigated system responses, MRR and R_a. The calculated values of F-ratio are compared to the critical Fisher value for a 95% confidence limit and the corresponding degree of freedom, $F_{(0.05;5;16)}$=2.85 and $F_{(0.05;10;16)}$=2.49. The obtained R-square coefficients for the developed models are about 97% for the MRR and 88% for R_a, ensuring an excellent fitting for the relationship between the process parameters and the investigated machining criteria.

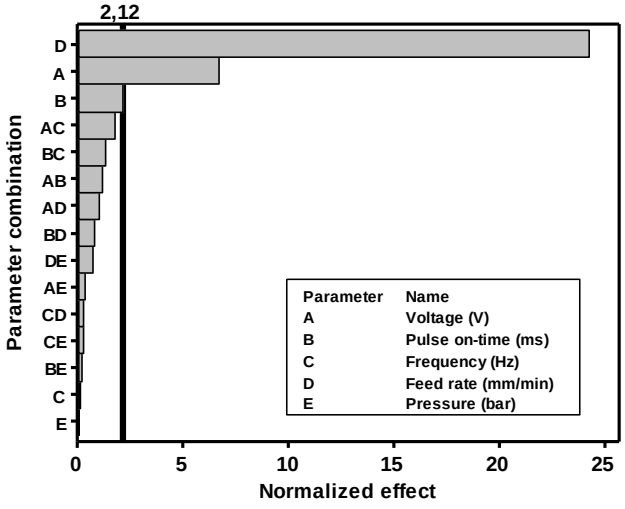

Figure 3 - Pareto chart applied to the MRR criteria

5.1 Analysis and optimization of MRR

As shown in Table 4, the F-value for the linear terms (127.31) is higher than the critical Fisher value $F_{(0.05;5;16)}$ whereas the F-value for the interaction terms (0.80) is smaller than the critical Fisher value $F_{(0.05;10;16)}$. This indicates that only the linear terms have significant influence on the MRR.

In order to highlight the most important causes of the total machining parameters and thus to optimize the developed model and to improve the polynomial fitting, the Pareto chart of the MRR is generated with Minitab 16 (Figure 3). The various parameter combinations are displayed against their normalized effect, i.e. the square root of their respective F-ratio value. The normalized effects which are higher than 2.12, i.e. the square root of the critical Fisher value $F_{(0.05;1;16)}$, refer to significant machining parameters.

Figure 3 indicates that only the cathode feed rate, the applied voltage and the pulse on-time have a significant influence on the MRR. According to Siebertz, Bebber and Hochkirchen [6], the non-significant effects can be eliminated from the existing model and a new improved and simplified model is developed. The new relationship obtained is given as follows:

$$MRR = 0.2019 + 0.0182X_1 + 0.0057X_2 + 0.0659X_4 \quad (4)$$

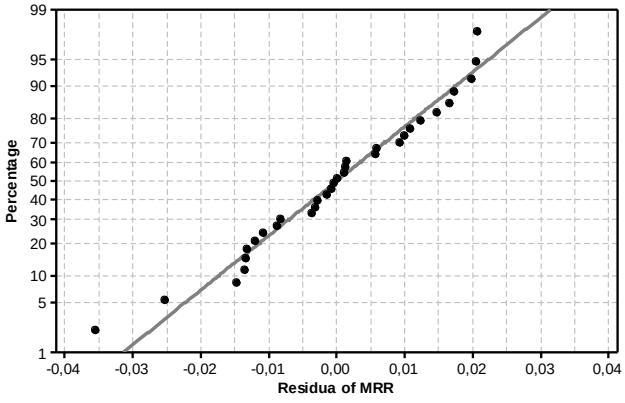

Figure 4 - Full-Normal Plot of the MRR-Residua

Source of variation	Degrees of freedom		Sum of squares		Mean sum of squares		F-value	
	MRR	R_a	MRR	R_a	MRR	R_a	MRR	R_a
Linear	3	5	0.150438	0.003988	0.050146	0.000798	247.74	3.79
Interaction	0	4	XXX	0.022726	XXX	0.003247	XXX	15.43
Error	28	19	0.005668	0.003997	0.000202	0.000210		
Total	31	31	0.156106	0.030711				

Table 5 - Analysis of variance of the improved model for the MRR and the R_a criteria

Levels of factors					Model		Experiment		$t_{calculated}$	
X_1	X_2	X_3	X_4	X_5	MRR (g/min)	R_a (µm)	MRR (g/min)	R_a (µm)	MRR	R_a
1	-1	0.5	0	-0.5	0.2144	0.1374	0.2091	0.1163	0.3691	1.4543
-0.5	-0.5	-0.5	-0.5	-0.5	0.1570	0.1418	0.2138	0.1209	0.8634	1.4436
0	0	0	0	0	0.2019	0.1463	0.1448	0.1307	0.4189	1.0747

Table 6 - Confirmation student's *t*-test results for MRR and R_a

The calculated final model was tested and confirmed by applying the analysis of variance, the F-ratio test (Table 5) and the student's *t*-test and by analysing the Full-Normal plot of the MRR-Residua.

The obtained $t_{calculated}$ values for MRR (Table 6) are smaller than the unilateral critical student t-value for a 95% confidence limit and the corresponding degrees of freedom ($t_{(0.05;28)}$=1.70) involving the model adequacy.

By the Full-Normal-Plot (Figure 4), a regression line is formed which exhibits systematic deviations between prediction and test results since purely random fluctuations follow a normal distribution [6]. As shown in Figure 4, the MRR-residua are normally distributed around the regression line. The absence of outliers indicates prediction accuracy.

5.2 Analysis and optimization of R_a

As shown in Table 4, both linear and interaction F-value terms (respectively 3.53 and 10.21) are higher than the critical Fisher values. This indicates that linear and interaction terms influence the R_a criteria.

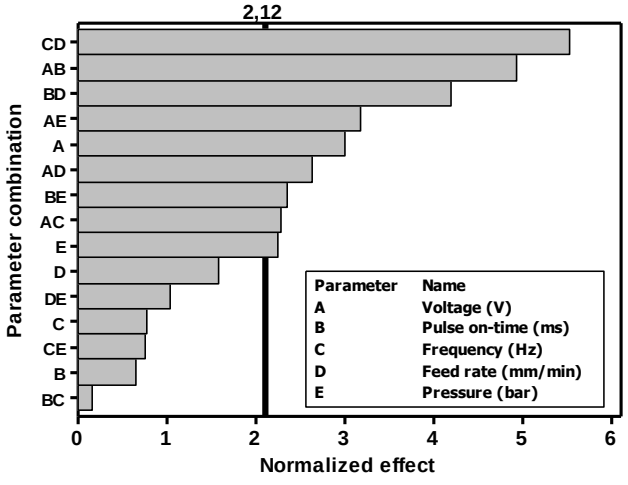

Figure 5 - Pareto chart applied to the R_a criteria

The Pareto chart of the R_a is generated (Figure 5) and highlights the parameter combinations which have significant influence on the R_a. According to Siebertz, Bebber and Hochkirchen [6], the non-significant effects can be eliminated, but the effects of the feed rate, the frequency and the pulse on-time cannot be eliminated since they occur in significant interactions. The obtained enhanced relationship is given as follows:

$$R_a = 0.1463 + 0.0080X_1 + 0.0017X_2 - 0.0021X_3 - 0.0042X_4 + 0.0060X_5 + 0.0131X_1X_2 + 0.0061X_1X_3 - 0.0070X_1X_4 + 0.0085X_1X_5 - 0.0112X_2X_4 + 0.0063X_2X_5 - 0.0147X_3X_4 \quad (5)$$

The obtained $t_{calculated}$ values for R_a (Table 6) are smaller than the unilateral critical student t-value for a 95% confidence limit and the corresponding degrees of freedom ($t_{(0.05;19)}$=1.73) involving the model adequacy.

Figure 6 shows only one outlier by the Full-Normal-Plot of the R_a-criteria. Otherwise, the residua distribution suggests a normal distribution which implies model prediction accuracy.

In conclusion, the model for R_a is validated and disposes of good prediction accuracy.

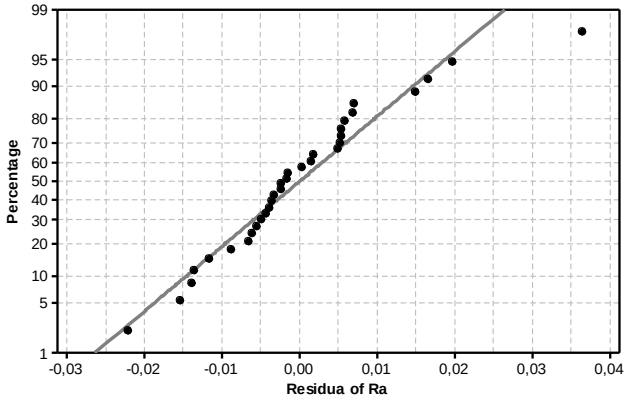

Figure 6 - Full-Normal Plot of the R_a-Residua

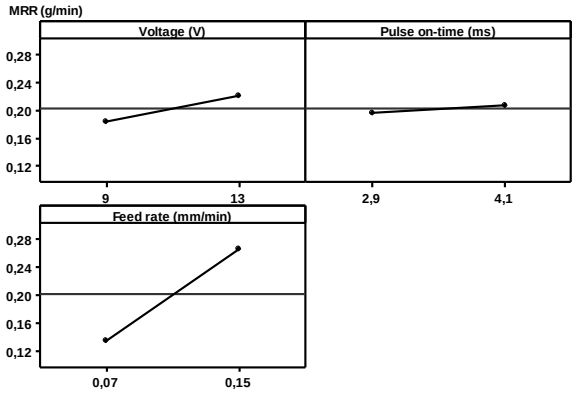

Figure 7 - Effect of parameter on MRR

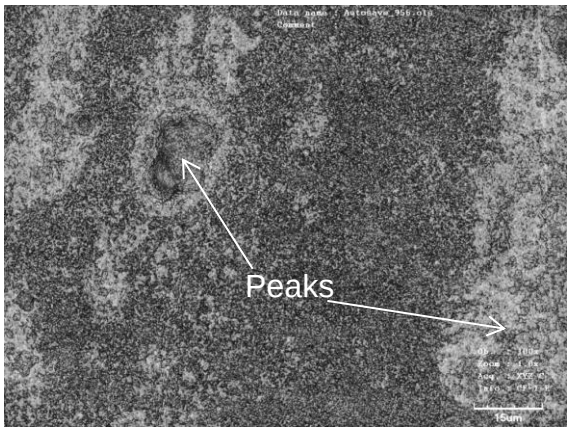

Figure 9 - Peaks occur at high voltage (13V)

6 RESULTS AND DISCUSSION

6.1 Effect of machining parameters on MRR

The mathematically developed model given by Eq. (4) enables the quantitative analysis of the considered process parameters on the MRR behaviour. From Figure 7 it can be noted that an increase in the cathode feed rate, the applied voltage or the pulse on-time leads to faster metal removal. This complies with the fundamental principles of metal removal in PECM [4], [5].

An increase in the feed rate implies a reduction of the interelectrode gap involving less ohmic resistance, i.e. more electrolyzing current and thus more anodic dissolution.

An increase in the potential leads to an increase in the current density in the interelectrode gap, involving a faster metal dissolution.

A longer pulse on-time implies more exchange of electric charges, i.e. more material removal.

6.2 Effect of machining parameters on R_a

Based on Eq. (5) as developed through the experimental observations and the Design of experiments methodology, studies of the effects of various process parameters and interaction on the surface roughness were carried out.

Figure 8 illustrates the effect of the linear terms on the R_a criteria. As shown in Figure 5, the pulse on-time, the vibration frequency of the cathode and the cathode feed rate do not strongly influence the surface integrity. Low pressure values lead to a better surface finish because a high pressure flow produces flow streaks which damage the surface thus reducing the generated finishing. An increase in the applied voltage leads to a deterioration of the microstructure (see Figure 9) diminishing the obtained surface roughness. In fact, higher voltage values imply higher current density which means different dissolution behaviours for the three principle material components, i.e. Fe, Ni and Co [8]. These different local oxidation ratios lead to inhomogeneous dissolution leading to an extreme poor surface finish.

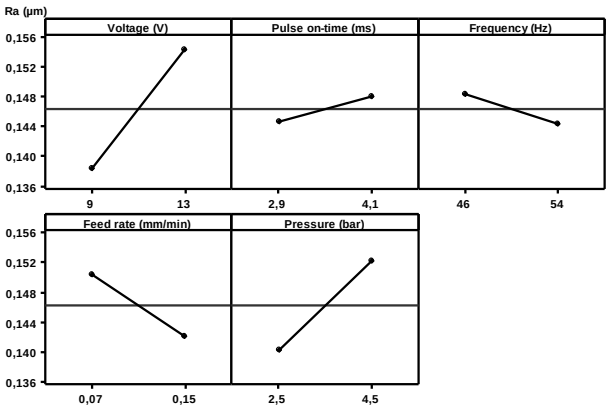

Figure 8 - Effect of parameters on R_a

6.3 The interactions as adjustment variables

Figure 10 exhibits the influence of the interaction terms on the machined surface. As demonstrated in Figure 5, the interactions X_2*X_3, X_3*X_5 and X_4*X_5 do not significantly influence the surface integrity.

The knowledge of the behaviour and of the variations of the interactions helps to optimize investigated criteria. In fact, as demonstrated in section 5.1, the feed rate does not significantly influence the R_a. Therefore, it should be hold at its high value to enhance the MRR. Besides, as the frequency does not influence MRR and R_a, the interaction between the feed rate and the frequency can be chosen in order to minimize the surface roughness. Thus, both criteria can be optimized.

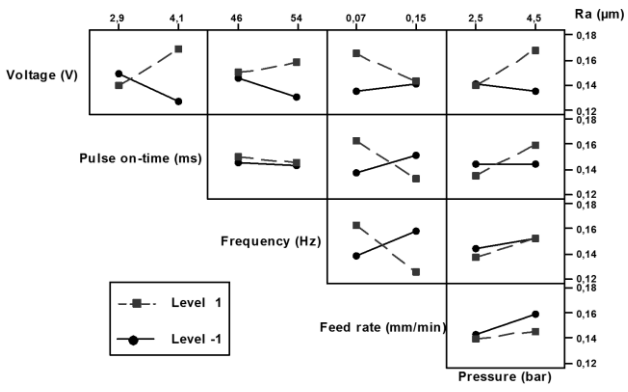

Figure 10 - Effect of parameter interactions on R_a

In the same way, as the pressure does not significantly influence the MRR (see section 5.1), a high voltage would improve the machining time and the selection of a low pressure/high voltage interaction could compensate the high voltage effect on the surface roughness.

7 CONCLUSIONS

The analysis of the experimental observations using the design of experiments methodology with a 2^k factorial plan has demonstrated the dependence of the investigated criteria, namely the material removal rate and the surface roughness, and the PECM process parameters considered in the present study (applied voltage, electric pulse on-time, cathode vibration frequency, cathode feed rate and electrolyte pressure).

The mathematical models developed on the basis of design of experiments have been found to be very powerful to predict the complex, linear and interactive effects of the various predominant machining variables on the investigated criteria as demonstrated in the analysis of variance. Besides, these formulations will not only help in analyzing the influence of the predominant process parameters, but they are also useful for the optimal search of various parametric combinations for achieving a maximum and faster fulfilment of the objective requirements of controlled PECM in practical applications.

The present results are profitable for both design and production engineers to assess the necessary information about MRR and R_a in PECM processes to achieve beneficial operational performance and low experiment costs.

The effective and efficient use of PECM technology for machining nickel-cobalt ferrous alloy to achieve the optimal combination of an enhanced metal removal rate and the generation of necessary surface integrity has been attempted.

8 ACKNOWLEDGEMENT

The authors gratefully acknowledge the European Regional Development Fund and the program INTERREG IVa for the financial support.

9 REFERENCES

[1] Rajurkar K.P., Zhu D., McGeough J.A., Kozak J., De Silva A., 1999, New development in electrochemical machining, Ann. CIRP, 48/2:567-579.

[2] Davis J. R., 2000, Nickel, cobalt, and their alloys, Materials Park, OH: ASM Internat.

[3] Zhang Y., 2010, Investigation into current efficiency for pulse electrochemical machining of nickel alloy, PhD-Thesis, University of Nebraska at Lincoln.

[4] Rajurkar K. P., Kozak J., Wei B., 1993, Study of pulse electrochemical machining characteristics, Ann. CIRP, 42/1:231-234.

[5] Moser S., 2004, Mikrostrukturierung von Metallen durch elektrochemischen Abtrag mit gepulstem Strom (PECM), PhD-Thesis, Heinrich Heine University Düsseldorf.

[6] Siebertz L., Van Bebber D., Hochkirchen T., 2010, Design of Experiments (DoE), Springer Heidelberg Dordrecht London New York.

[7] Das M.N., Giri N.G., 1986, Design and Analysis of Experiments, 2nd ed., Wiley, New York.

[8] Walther B., Schilm J., Michaelis A., Lohrengel M.M, 2007, Electrochemical dissolution of hard metal alloys, Electrochim. Acta, 52/27:7732-7737.

10 BIOGRAPHY

Dirk Bähre obtained his PhD degree in Production Engineering from the Technical University of Kaiserslautern. In 2008 he was appointed Professor in Production Engineering at Saarland University, Germany.

Olivier Weber obtained his master degree in Mechanical Engineering from both the Arts-et-Métiers ParisTech and the Karlsruhe Institute of Technology. He is currently a doctoral fellow at the Institute of Production Engineering at Saarland University and research engineer at the Center for Mechatronics and Automatization.

Andreas Rebschläger obtained his master degree in Mechatronics from Saarland University. He is currently a doctoral fellow at the Institute of Production Engineering at Saarland University and research engineer at the Center for Mechatronics and Automatization.

Philipp Steuer obtained his master degree in Mechatronics from Saarland University. He is currently a doctoral fellow at the Institute of Production Engineering at Saarland University and research engineer at the Center for Mechatronics and Automatization.